Chapter 4

The experimental system.

The whole system is sketched in Fig. 4.1. It consists in the light source, the sample cell and the image forming, capturing and processing system. In the first sections we describe all these parts and the criteria we followed to build our NFS instruments. In Sections 4.7 and 4.8 we describe the three NFS instruments we built.

4.1 The optical system.

The optical system is mainly built using elements supplied by Newport. The optical table is a VH3048 IsoStation. All the elements are mounted on X26 rails, by using CN26 carriers. A picture of the system is shown in Fig. 4.2.

For the experiment descibed in Chapter 9, the optical axis must be vertical. The X26 rails are held in vertical position by mounting them on an X95 rail with suitable carriers: see Fig. 4.3.

4.2 The light source.

The light source we use is a LED laser, coupled to a single mode fiber, supplied by Newport. In Tab. 4.1 we show the data supplied with the LED. Figure 4.4 shows the LED laser and the fiber.

The LED is housed in a Newport 700P temperature controller mount, connected to a temperature controller and a current driver. Since the output wavelenght depends on the temperature, a temperature controller is needed. The LED laser has a built-in monitoring photodiode. The current driver monitors the output power to keep it constant.

A single mode fiber is directly pigtailed to the LED. The other end of the fiber is terminated by an FC/PC connector. It is held by a Newport SL50BM, a gimbal mount for the adjustment of the azimuth and elevation, originally built for mounting mirrors or beam splitters. The beam output by the fiber is diverging; we collimate it by sending it through a lens with a focal of 5cm.

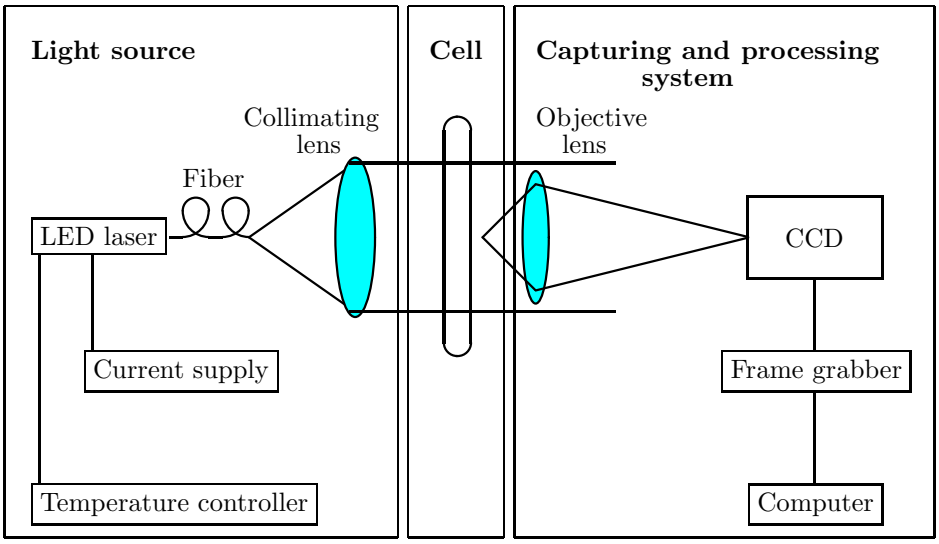

Figure 4.1: The experimental system.

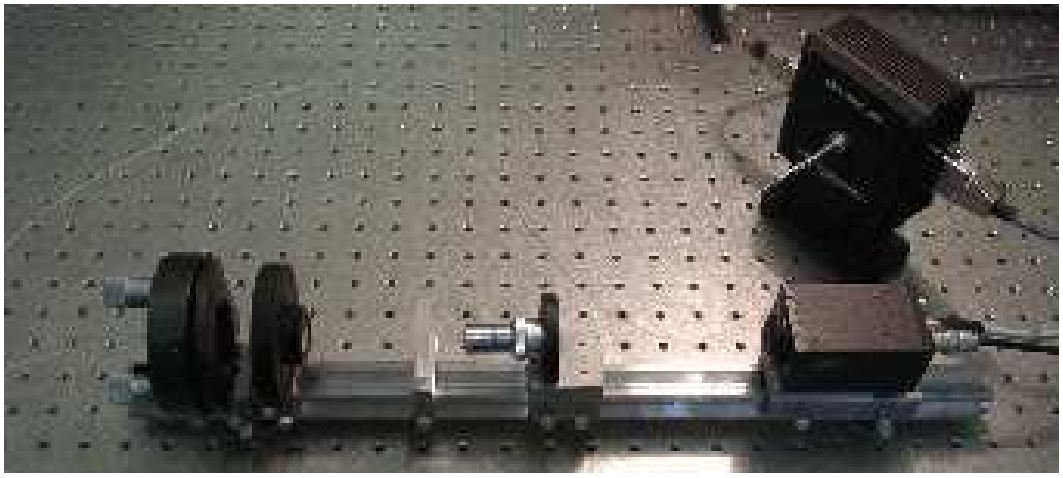

Figure 4.2: Picture of the optical system. From left to right, we can see the adjustable mount that holds the fiber, the collimating lens, the cell, the microscope objective and the CCD camera. In the upper right corner there's the laser mount.

Figure 4.3: A view of the optical system for the experiment described in Chapter 9. All the optical elements are alligned in vertical direction. From the bottom, we see the optic fiber, held by an adjustable mount, the collimating lens, the cell, held by the column on the left, the focusing lens, the blade, the neutral filter, and the CCD camera.

Item code	LD-635-31A
Center wavelength	635nm
Wavelength range	$\pm$10nm
Fiber output power	1.2mW
Threshold current	10mA
Operating current	40mA
Rise/fall time	1.5ns
Operating temperature	-10 to 40°C
Fiber core/clad diameter	4/125μm - single mode

Table 4.1: Data of the LED laser.

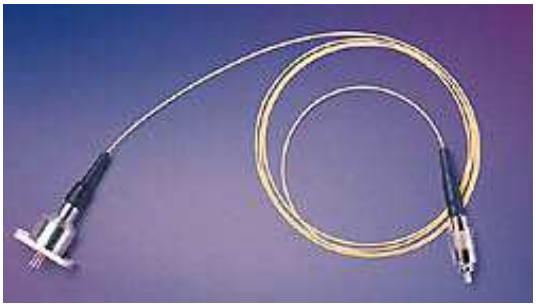

Figure 4.4: The LED laser.

The resulting beam has a diameter of about 2cm. This diameter is enough for our experiments; in general, it must be selected as a function of the wavevector range $[q_{min}, q_{max}]$ we want to measure. For ONFS and ENFS, D, the diameter over which the beam intensity is constant, must be selected in order to fulfill Eq. (3.64). The best choice is:

$$D \gtrapprox 50\frac{q_{max}}{q_{min}^2} \tag{4.1}$$

For SNFS, the beam must have a diameter which covers a good statistical sample:

$$D \gtrapprox 20/q_{min}. \tag{4.2}$$

Both the adjustment of the direction of the beam and its collimation are not critical operations. The direction of the beam must be adjusted to hit a lens, centered at the optical axis, half a meter away from the fiber end. The collimation is checked by measuring the beam diameter on a screen, near the lens and one meter away. The collimator is shown in Fig. 4.5.

The LED laser has been used in order to test its performance for industrial applications. The LED laser is much more compact and robust than a gas laser; it can operate immediately after it has been powered on and it does not generate too many heat. For these features it is ideally suited for industrial applications. Moreover, the overall cost of a LED laser device included in an industrial product can be made extremely low, as in the case of CD readers, though a laboratory LED laser equipement can cost as much as a classical gas laser. Moreover, the output of a gas laser must be spatially filtered before being used. A spatial filter is a critical component in an industrial equipement, since it must be extremely stable, and must be adjusted by micrometric actuators controlled by sensors, in order to correct the deformations due to heating and mechanical stresses. On the contrary, the single mode fiber output is more uniform than the output of a spatial filter, and requires no adjustment.

4.3 The cell.

The liquid samples we measure are held in a cell; the diameter D must be selected following Eq. (4.1) for ONFS and ENFS, or Eq. (4.2) for SNFS.

For homogeneous samples, like colloids, the thickness must be selected in order to have a suitable attenuation of the main beam, about 1%. For ONFS measurements, the thickness of the cell and the volumetric particle density must fulfill Eq. (3.63); generally this condition is spontaneously met.

For ONFS and ENFS measurements, the parallelism between the windows of the cell is not critical, nor the optical quality of them. Since the measured scattered light comes from different regions of the sample, we must provide that it is homogeneous. This implies that the thickness must be uniform, but an optical quality allignment is far beyond what is needed. On the contrary, SNFS requires optical quality windows: the well known "Foucault test" sees every deformation of the wavefront, no matter if the associated wavelength is long.

Figure 4.5: A view of the collimator and the cell. From the bottom, we see the optic fiber, held by an adjustable mount, the collimating lens, and the cell.

The cells we used are described in detail in Chapters 7 and 9.

4.4 Objective, beam stop and blade.

The objective must form an image of a given plane on the CCD sensor. The magnification M must be selected in order that the required wavevector range $[q_{min}, q_{max}]$ is inside the wavevector range the CCD sensor can measure: about $\left[2 \times 10^3 \mathrm{m}^{-1}, 2 \times 10^5 \mathrm{m}^{-1}\right]$. This means that:

$$\left[\frac{q_{min}}{M}, \frac{q_{max}}{M}\right] \subseteq \left[2 \times 10^3 \mathrm{m}^{-1}, 2 \times 10^5 \mathrm{m}^{-1}\right] \tag{4.3}$$

Moreover, the numerical aperture of the lens must be enough to resolve details as small as the smallest wavelength involved, $2\pi/q_{max}$, or, equivalently, to collect light scattered at an angle q_{max}/k.

In our experiments, we used a 20X microscope objective for high magnification factors, and an achromatic, 10cm focal length doublet for magnification factor around 1. An achromatic doublet has also been tested for high magnification factors, since we do not require the high quality of a microscope objective, nor an extremely wide numerical aperture. Experiments proved no different performances of the doublet compared with the microscope objective, but it was more difficult to obtain the required magnification.

The objective lens must be placed so that it creates an image of a given plane on the CCD sensor. For ONFS and ENFS, the plane must be at a distance z from the sample fulfilling Eq. (3.60). The best choice is:

$$z \approx 25 \frac{k}{q_{min}^2} \tag{4.4}$$

For SNFS:

$$z < \frac{kD}{2q_{max}} \tag{4.5}$$

For ONFS, the transmitted beam, focused by the objective, is stopped by an opaque or reflective element. In microscope objectives, the focal plane is inside, between two groups of lenses: we insert the beam stop through a hole. We tried three kinds of beam stops: a thin wire, a reflective wedge and an absorbing disc impressed by on a photographic film. The wire has a diameter of 70μm; it si stretched in the focal plane and is positioned by micrometric screws. It reflects the light inside the objective, and this could, in principle, increase the stray light. The photographic film we used are high contrast, black and white, 36mm photographic films. The beam stop is circular, but the beam is not completely blocked, thus increasing the stray light. The wedge was obtained by a steel blade; the edge was kept parallel to the optic axis. The upper part, in the direction from which the light comes, was cut at 45° and polished, in order to obtain a surface that reflects the main beam outside the lens mount, through a second hole. A section of the objective lens is shown in figure (4.6). This kind of beam stop is not symmetrical with respect to the optical axis. This

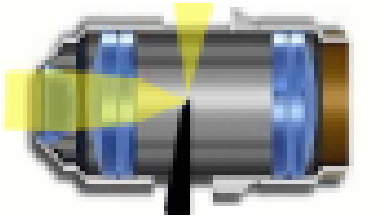

Figure 4.6: Section of the microscope objective and the beam stop.

could increase the difficulty to process the data. During the experiments, all the methods showed to be almost equivalent. Figure 4.7 shows the mount that holds the beam stop.

For SNFS, a blade must be placed in the plane where the transmitted beam is focused. The blade must be extremely sharp: a razor blade is required. We mount it on a system with three micrometric screws, in order to accurately position it in the space. A picture of the Schlieren system is shown in Fig. 4.8.

4.5 CCD sensor.

We used an industrial CCD camera: JAI CV M50. An image is shown in Fig. 4.9; the data are provided in Tab. 4.2.

The output is a standard CCIR; since it is interlaced, an image is alwais formed by two fields acquired with a time delay of 0.04s, although the internal shutter allows to acquire a single frame in 100ns.

The number of pixels and their dimension determine the wavevector range the CCD can directly measure: $\left[2 \times 10^3 \mathrm{m}^{-1}, 2 \times 10^5 \mathrm{m}^{-1}\right]$. Other wavevector ranges can be covered, by creating on image with a suitable magnification factor, but we cannot cover more than two decades.

4.6 The acquisition and elaboration system.

The frame grabber we used is an IC-RGB, from Imaging Technology. It performs an 8 bit digitalization of three standard composite video signals from the CCD cameras. It can be used to acquire simultaneously from two syncronized CCD cameras, for evaluating the intensity correlation function on two different planes, or to acquire from a single camera.

The syncronyzed acquisition from two cameras can be used to evaluate the three dimensional correlation function; the meaning of the three dimensional correlation function is explained in Appendix A.

The software for image elaboration was developed under Linux, written in C language. The drivers and the libraries are the “IC-PCI” provided by “GOM Optical Measurements Techniques”. The algorithms used to process the images are described in Chapt. 5 and 6.

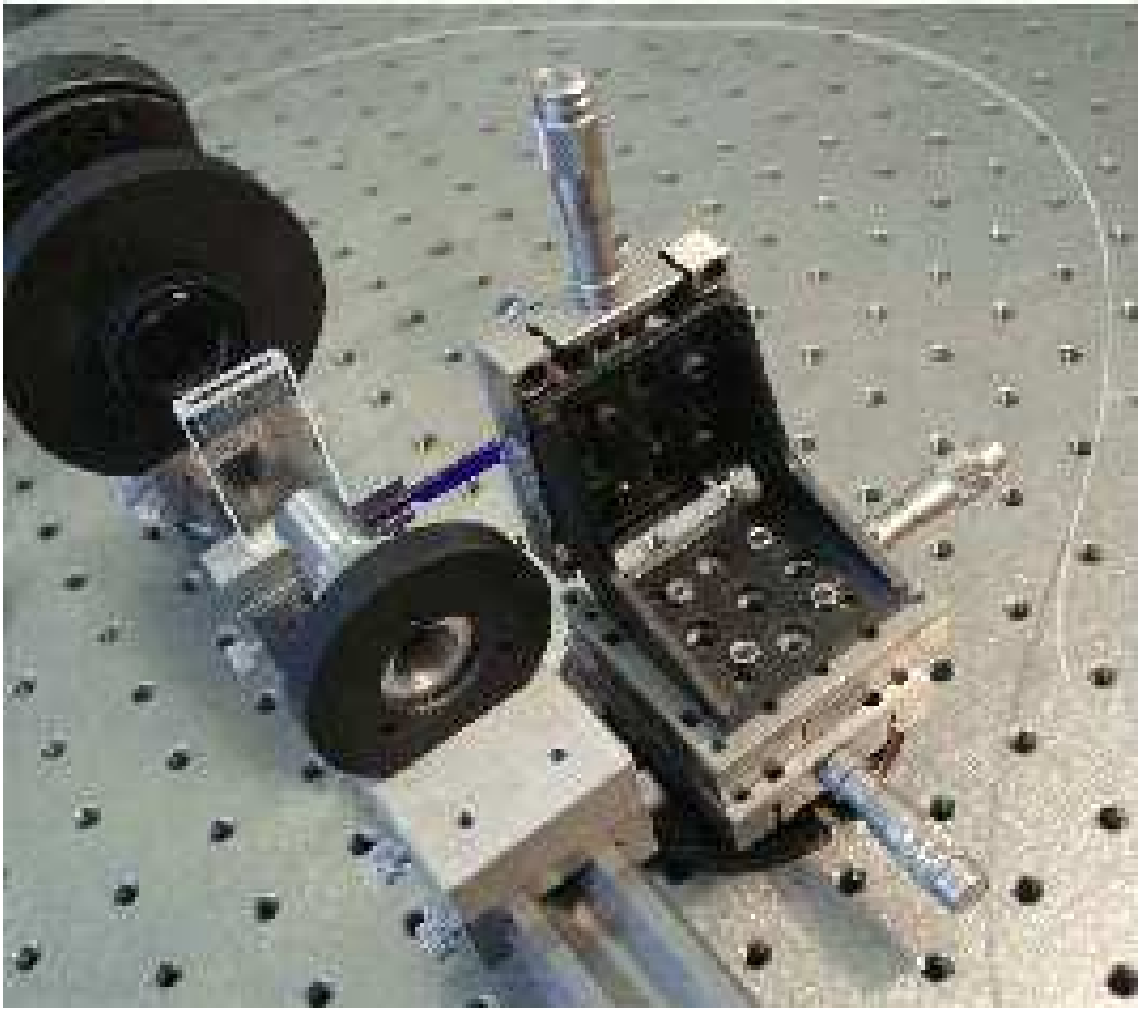

Figure 4.7: Picture of the microscope objective with the beam stop. The beam stop is glued to the blue rod, held by a mount with three micrometric screws, for the adjustment of the position in every direction.

Figure 4.8: A view of the Schlieren system. From the bottom, we see the cell, the focusing lens, the blade, held by a micrometric mount, the neutral filter and the CCD camera.

Specifications	CV-M50C
Scanning system	625 lines 25 frames/s
CCD Sensor	Monochrome 1/2" Hyper HAD IT CCD
Sensing area	6.6mm×4.8mm
Picture elements effective	752×582
Elements in video out	737×575
Cell size	8.6×8.3
Resolution (horizontal)	560 TV lines
Resolution (vertical)	575 TV lines
Sensitivity	0.5 lux, f1.4
Sensitivity peak wave length	500nm
Wave length range	400nm - 675nm (sensitivity > 50%)
S/N ratio	>56dB (AGC off, Gamma 1)
Video output	Composite VBS Signal 1.0 V_{pp}, 75 Ω
Gamma	0.45 - 1.0
Gain	Manual - Automatic
Scanning	2:1 interlace
Accumulation	Field - Frame
Syncronization	Internal, Xtal-generated - External HD/VD - random trigger
HD Sync input - output	4V, 75 Ω
VD Sync input - output	4V, 75 Ω
Trigger input	4V, 75 Ω
Trigger input duration	> HD interval
WEN output (write enable)	4V, 75 Ω
EEN output (exposure enable)	4V, 75 Ω
Pixel clock out (optional)	4V, 75 Ω
Internal shutter	Off,1/100s, 1/250s, 1/500s, 1/1000s, 1/2000s, 1/4500s, 1.10000s
Trigger shutter	1/60,1/100s, 1/250s, 1/500s, 1/1000s, 1/2000s, 1/4500s, 1.10000s
Long time exposures	one field to $+\infty$. Duration between external VD pulses.
Operating temperature	-5°C to +45°C
Humidity	20%-80% non-condensing
Storage temperature	-25°C to +60°C
Storage humidity	20%-90%
Power	12V DC ±10% 2.5W
Lens mount	C-mount
Dimensions	40mm×50mm×80mm
Weight	245g

Table 4.2: Specification of Jai CV M50C camera.

Figure 4.9: Jai CV M50 camera.

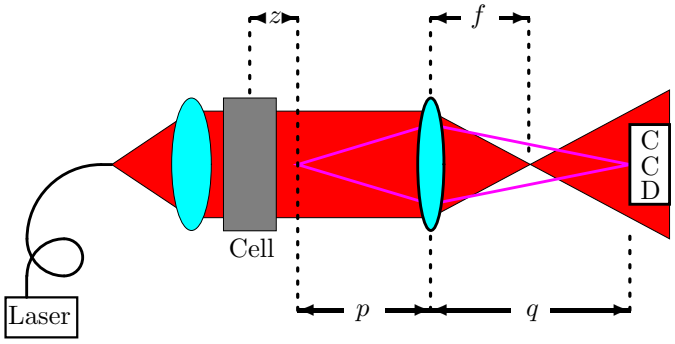

Figure 4.10: The optical setupt for the measurement of scattering from colloids some microns large with ENFS.

4.7 ONFS and ENFS setup for colloid measurements.

The systems are sketched in Figs. 4.10 and 4.11.

The measurements described in Chapters 7 and 8 cover the wavevector range $[q_{min}, q_{max}]$ about $\left[2 \times 10^5 \mathrm{m}^{-1}, 4 \times 10^6 \mathrm{m}^{-1}\right]$. By using Eqs. (4.1) and (4.4), we obtain $D \gtrapprox 5$mm and $z \approx 6$mm. A 2cm beam diameter, obtained with lenses with 25mm diameter, as shown in Fig. 4.2, is enough to ensure that the intensity is constant over the length D. For the measurements described in Chapters 7 and 8, we used larger lenses with 50mm diameter, with a larger beam diameter, in order to ensure a better uniformity, and z was increased acordingly.

Following Eq. (4.3), we obtain the magnification: $M = 20$. We used a 20X microscope objective and numerical aperture of 0.45.

The whole optical system for ENFS is shown in Fig. 4.2.

For ONFS, we insert a beam stop through a hole inside the lens mount. The beam stop and its adjustable mount is shown in Fig. 4.7.

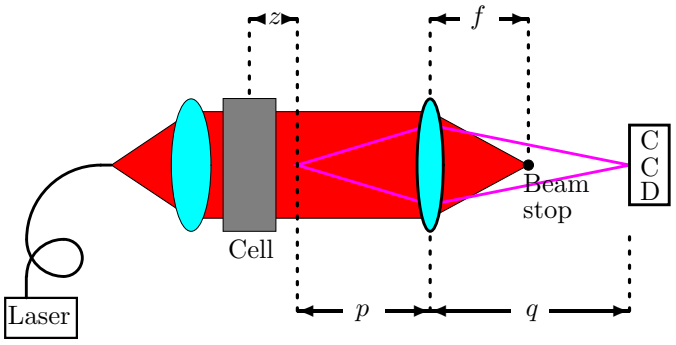

Figure 4.11: The optical setupt for the measurement of scattering from colloids some microns large with ONFS.

4.8 SNFS setup for non equilibrium fluctuation measurements.

The overall system is sketched in Fig. 4.12.

The range $[q_{min}, q_{max}]$ of the fluctuations we measure is about $\left[2 \times 10^3 \mathrm{m}^{-1}, 2 \times 10^5 \mathrm{m}^{-1}\right]$, that is, the fluctuations range from ten microns to some millimeters. By using Eqs. (4.2) and (4.5), we obtain $D \gtrapprox 10\mathrm{mm}$ and $z < 125\mathrm{mm}$. The cell we used, described in Chapter 9, has an internal diameter of about 25mm.

Following Eq. (4.3), we obtain the magnification: $M = 1$. We used an achromatic doublet with a 25mm diameter and focal length $f = 100\mathrm{mm}$. To obtain the required magnification, $p = q = 200\mathrm{mm}$. Since SNFS is affected by small inhomogeneous fluctuations of air temperature, we choose to put the collimating lens and the objective lens as close as possible to the cell, in order to prevent air movements. This resulted in a negative z.

The whole optical system is shown in Fig. 4.3.

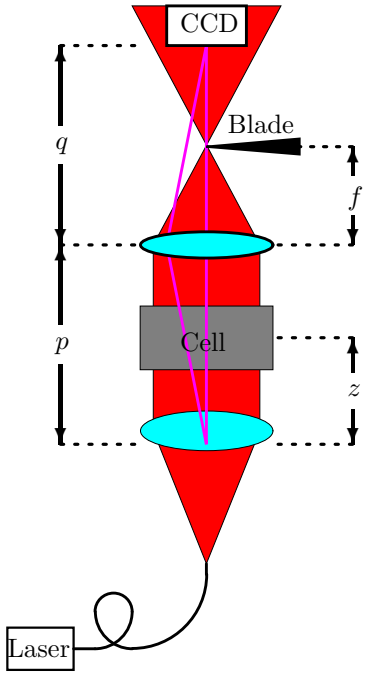

Figure 4.12: The optical setupt for the measurement of non equilibrium fluctuations with SNFS.